Role of hydrogen on the deposition and properties of fluorinated silicon-nitride films prepared by inductively coupled plasma enhanced chemical vapor deposition using $SiF_4/N_2/H_2$ mixtures

J. Fandiño and G. Santana
Instituto de Investigaciones en Materiales, Universidad Nacional Autónoma de México, Ciudad Universitaria, Coyoacán 04510, México D.F., Mexico

L. Rodríguez-Fernández and J. C. Cheang-Wong
Instituto de Física, Universidad Nacional Autónoma de México, Ciudad Universitaria, Coyoacán 04510, México D.F., Mexico

A. Ortiz and J. C. Alonso
Instituto de Investigaciones en Materiales, Universidad Nacional Autónoma de México, Ciudad Universitaria, Coyoacán 04510, México D.F., Mexico

(Received 26 August 2004; accepted 6 December 2004; published 2 February 2005)

Fluorinated silicon-nitride films have been prepared at low temperature (250 °C) by remote plasma enhanced chemical vapor deposition using mixtures of SiF_4, N_2, Ar, and various H_2 flow rates. The deposited films were characterized by means of single wavelength ellipsometry, infrared transmission, resonant nuclear reactions, Rutherford backscattering analysis, and current-voltage measurements. It was found that films deposited without hydrogen grow with the highest deposition rate, however, they result with the highest fluorine content (~27 at. %) and excess of silicon (Si/N ratio≈1.75). These films also have the lowest refractive index and the highest etch rate, and exhibit very poor dielectric properties. As a consequence of the high fluorine content, these films hydrolize rapidly upon exposure to the ambient moisture, forming Si–H and N–H bonds, however, they do not oxidize completely. The addition of hydrogen to the deposition process reduces the deposition rate but improves systematically the stability and insulating properties of the films by reducing the amount of both silicon and fluorine incorporated during growth. All the fluorinated silicon-nitride films deposited at hydrogen flow rates higher than 3.5 sccm resulted free of Si–H bonds. In spite of the fact that films obtained at the highest hydrogen flow rate used in this work are still silicon rich (Si/N ratio≈1.0) and contain a considerable amount of fluorine (~16 at. %), they are chemically stable and show acceptable dielectric properties. © *2005 American Vacuum Society.* [DOI: 10.1116/1.1854693]

I. INTRODUCTION

Amorphous silicon-nitride thin films have a large spectrum of applications in the fabrication of microelectronic and optoelectronic devices, such as gate dielectric layers in MIS and thin-film transistors, diffusion barriers in multilayer devices, final passivation films in semiconductor devices, protective and antireflecting coatings in solar cells, etc. The increasing technological advancements and the scaling down of the sizes of modern microelectronic devices have imposed the necessity of lowering the deposition temperatures of these films.[1,2] For applications in hydrogenated amorphous silicon (a-Si:H) devices, this requirement is also fundamental to avoid the effusion of hydrogen from the a-Si:H films, which degrades their electrical properties.[3–5] Silicon nitride films deposited by conventional direct plasma-enhanced chemical-vapor deposition (PECVD) using SiH_4 as the silicon precursor gas and NH_3 or N_2 as nitrogen source gas meet quite well the requirement of low-temperature processing.[6–12] However, the dielectric integrity and stability of these films is usually affected by the incorporation of Si–H bonds.

Some approaches proposed to reduce the Si–H content in plasma deposited silicon nitride films make use of SiH_4 and modified plasma techniques such as remote-PECVD (RPECVD),[1,3,13–15] electron cyclotron resonance PECVD (ECR-PECVD),[16–18] inductively coupled plasma CVD (ICP-CVD).[19] Other strategies, proposed since more than one and a half decades ago, have been based on the use of conventional or modified PECVD processes in combination with alternative silicon ($SiF_4, SiF_2, Si_2F_6, SiH_2F_2, SiH_2Cl_2$)[20–27] or nitrogen sources (NF_3).[28–33] These approaches give rise to fluorinated or chlorinated silicon nitrides, in which the concentration of Si–H bonds can be drastically reduced, or even eliminated by increasing the amount of the halogenated source introduced in the process mixture. Due to the higher bond energy of the Si–F (131.9 kcal/mol) and Si–Cl (109 kcal/mol) bonds, compared with that of the Si–H (71.5 kcal/mol) bonds,[34] halogenated silicon nitride films have in general better thermal, chemical, and electrical stability than hydrogenated silicon nitride films. However, it has been generally found that films with a large halogen content have a very open structure, hydrolyze and oxidize rapidly, and can even be converted

into silicon dioxide.[20,24,28,30,32] Therefore one problem to address with the use of halogenated sources for PECVD deposition of silicon nitride films is to achieve good control and/or to minimize the incorporation of halogen atoms.

Some of the most recent reports have shown that high quality fluorinated silicon nitride films can be obtained at low temperatures by REPCVD using mixtures of SiF_4 and NH_3.[27] Under this approach, the control of the fluorine concentration in the films is achieved by changing the NH_3/SiF_4 ratio, because the hydrogen coming from NH_3 acts as a gettering agent to extract fluorine from the film forming reactions. In spite of this achievement, one apparent limitation of this approach is that fluorine concentration can not be varied independently of the ratio of N to Si atoms incorporated in the film. Due to this we were motivated to investigate the deposition and resulting properties of fluorinated silicon nitride films prepared by high density–inductively coupled RPECVD from $Ar/SiF_4/N_2/H_2$ mixtures, with particular emphasis on the study of the role of the hydrogen flow rate on the deposition rate, fluorine content, and properties of the films. In principle the use of this mixture has the advantage of having separated the hydrogen source from the nitrogen source, which should allow the control of fluorine incorporation independently of the N/Si ratio incorporated in the film. Another potential advantage previewed for the use of this mixture is the possibility to reduce the incorporation of N–H bonds.

II. EXPERIMENT

The films were deposited in a custom designed RPECVD system manufactured by MVSystem (Colorado), whose characteristics have been reported elsewhere.[27] Ar and N_2 were fed into the chamber from the top of the quartz tube (plasma region), meanwhile SiF_4 and H_2 were fed downstream to the plasma by means of the dispersal rings located a few centimeters over the substrate holder. All the films were deposited at a constant substrate temperature of 250 °C, and the rf power was fixed at 550 W giving a power density of 7 W cm^{-2}. The flow rates of Ar, SiF_4, and N_2 were kept constant at values of 38, 3.5, and 7.0 sccm, respectively. The main variable in this study was the hydrogen flow rate, which took values from zero (0), to 21 sccm. The working pressure was fixed at 10 mTorr by adjusting the pumping speed of the turbomolecular pump.

In order to make the structural characterization, films approximately 100 and 500 nm thick were grown on (100) *n*-type silicon crystalline substrates with a resistivity of 200 Ω cm. Prior to deposition, the substrates were cleaned by immersion in "*p*-etch solution" (300:15:10 parts of $H_2O:HNO_3:HF$) for 5 min.

The thickness and refractive index of the films were determined by ellipsometric measurements, carried out with a null single wavelength Gaertner L117 ellipsometer at 632.8 nm. Infrared transmission spectra were obtained *ex situ* by means of a Fourier transform infrared (FTIR) Nicolet 210 spectrophotometer, operated in the range of 400–4000 cm^{-1}, with 8 cm^{-1} in resolution in order to avoid interference effects.

The total amount of fluorine atoms in the films was measured with the resonant nuclear reaction (RNR) technique[35] using the Instituto de Física 700 kV Van de Graaff accelerator. Following this procedure the amount of F atoms is determined by the number of gamma rays produced from the $^{19}F(p,\alpha\gamma)^{16}O$ nuclear reaction, taking advantage of its sharp resonance at a proton bombarding energy of 340 keV. In our experiments, a 5.1-cm-diam by 5.1-cm-thick NaI(Ti) scintillation detector (placed as close as possible to the sample) was used to detect the γ rays emitted in the forward direction (0° laboratory angle). The excitation curves of the $^{19}F(p,\alpha\gamma)^{16}O$ nuclear reactions were obtained automatically using a computer program[36] and each measured point corresponded to a dose of 5 μC. Quantification of the atomic fraction of fluorine in the Si_3N_4 films was made by comparison of the gamma yield Y_F from our samples with that of a reference standard Y_S having a known atomic fraction f of fluorine.[35,37] In the present case, a thick LiF crystal was used as a reference standard. Rutherford backscattering spectrometry (RBS) was used to determine the elemental composition of the films. These experiments were performed using the 3 MV tandem accelerator (NEC 9SDH-2 Pelletron) of the Instituto de Física. In particular, with a ^4He beam we took advantage of the elastic $^{16}O(\alpha,\alpha)^{16}O$ scattering resonance at 3.045 MeV for the oxygen measurements. At this resonant energy, the cross section for oxygen is 25 times larger than its corresponding Rutherford cross section, allowing high sensitivity for oxygen content determination.[38] The film composition was then determined by fitting the experimental RBS spectra using the RUMP simulation program.[39]

The electrical properties of some fluorinated silicon nitride films ($SiN_x:F$) were assayed from current-voltage measurements carried out on aluminum/$SiN_x:F$/silicon structures. The metal insulator silicon (MIS) structures were constructed by evaporating aluminum discs with an area of 0.013 cm^2 on $SiN_x:F$ films on *n*-type (100), 0.1–2.0 Ω cm, single crystalline silicon substrates, previously cleaned with the RCA process. The *I-V* measurements were obtained using a Keithley 230 voltage source and a Keithley 485 picoameter, both programmable, applying a ramp voltage of 0.5 V s^{-1}.

III. RESULTS

Figure 1 shows the variation in film growth rate and refractive index as a function of the hydrogen flow rate used during the deposition process. As can be seen from this figure, the highest growth rate (14 nm/min) is obtained for films deposited without hydrogen, and this rate decreases with the addition of hydrogen. Figure 1 also shows that all the films have refractive index values lower than the value corresponding to the stoichiometric material (2.0), which is characteristic of fluorinated silicon nitride films. The lowest refractive index value (1.6) corresponds to the film deposited without hydrogen, and it increases asymptotically toward 1.72 as the hydrogen flow rate increases from 0 to 21 sccm.

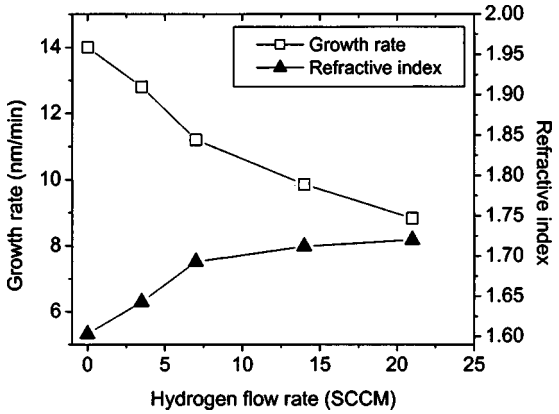

FIG. 1. Growth rate and refractive index vs hydrogen flow rate for fluorinated silicon-nitride films deposited by RPECVD using $SiF_4/N_2/H_2/Ar$ mixtures.

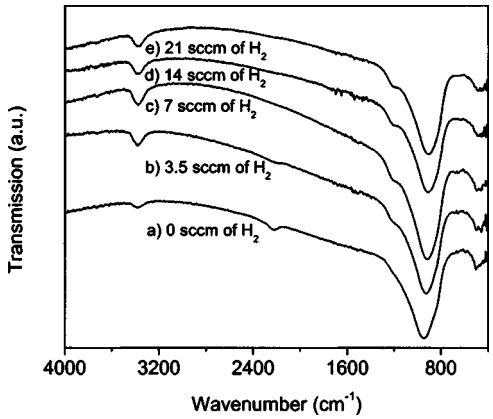

FIG. 3. FTIR spectra of fluorinated silicon-nitride films with hydrogen flow rate as a parameter: (a) 0 sccm, (b) 3.5 sccm, (c) 7 sccm, (d) 14 sccm, (e) 21 sccm.

The behavior of the etch rate of the films in the 5% HF buffer solution as a function of hydrogen dilution is shown in Fig. 2. Films prepared without hydrogen have the highest etch rate (9.2 nm/s) and as hydrogen is added to the reactions the etch rate decreases, reaching a minimum value of 2 nm/s. Typical FTIR transmission spectra of films deposited under the different H_2 flow rates are shown in Fig. 3. In all the spectra clearly appears a broad and intense absorption band centered around 900–945 cm^{-1}, as well as a small peak around 475–495 cm^{-1}, which can be associated to the asymmetric stretching of Si–N bonds and Si breathing vibrations in the fluorinated silicon nitride films, respectively.[20–24,27,28,40] The absorption due to Si–F bonds (810–1050 cm^{-1}) and N–F bonds (1032 cm^{-1}), if they exist, are veiled by the wide Si–N absorption band.[22,27,28,41,42] There are also absorption peaks, at 3378 and 1200 cm^{-1} related to stretching and bending vibrations of N–H bonds, respectively.[20–24,27,28] Additionally, a small absorption band located at 2219 cm^{-1}, related to Si–H bonds,[23,29,31,43–46] is observed in the spectra of the films deposited without hydrogen and with a low hydrogen flow rate (3.5 sccm), although in the latter case the intensity is low. There was no absorption band related to Si–H bonds for films deposited at hydrogen flow rates larger than 3.5 sccm. It is worth mentioning that the infrared spectra shown in Fig. 3 were obtained *ex situ* just after taking out each sample from the deposition chamber. This was done in order to minimize the exposure time of the samples to ambient moisture. The stability of the samples under exposure to the ambient air and moisture were systematically studied by taking infrared spectra and measuring their refractive index after different intervals of time. No changes were detected in the infrared characteristics and refractive index of any of the samples, even after a period of 3 months. In order to make a further test of the chemical stability of the films they were immersed in de-ionized water for 168 h. After this accelerated oxidation test, no changes were found in the FTIR spectra and refractive index. The comparative analysis among IR spectra shows that the absorption peak related to Si–N bonds gradually shifts toward lower wave numbers as the amount of hydrogen increases. The plot of the peak position of this fundamental absorption band as a function of H_2 flow rate is depicted in Fig. 4. As can be seen in this plot, the wave number of this peak decreases from approximately 945 to 900 cm^{-1} as the hydrogen flow rate increases from 0 to 21 sccm.

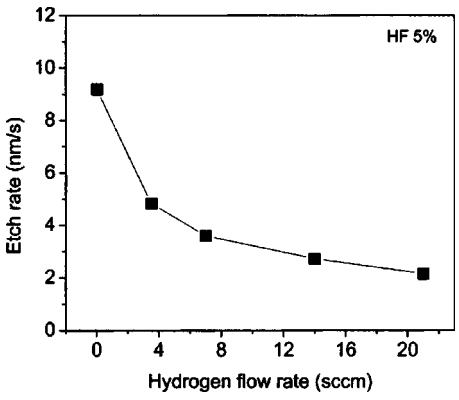

FIG. 2. Etch rate of fluorinated silicon-nitride films as a function of hydrogen flow rate.

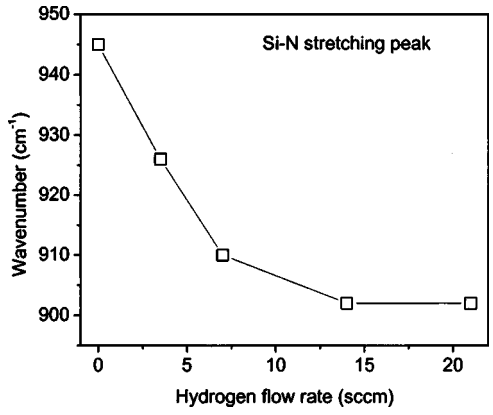

FIG. 4. Fundamental Si–N stretching (FTIR) peak position for the films as a function of hydrogen flow rate.

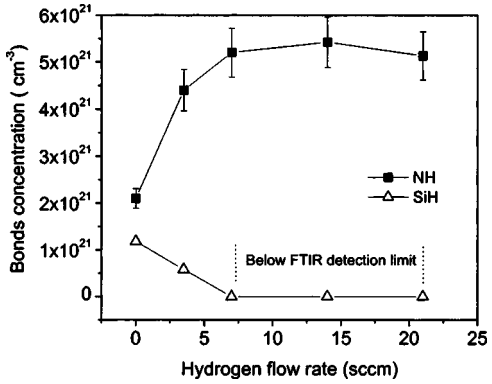

FIG. 5. Concentration of Si–H (△) and N–H (■) bonds in films deposited under the various hydrogen flow rates.

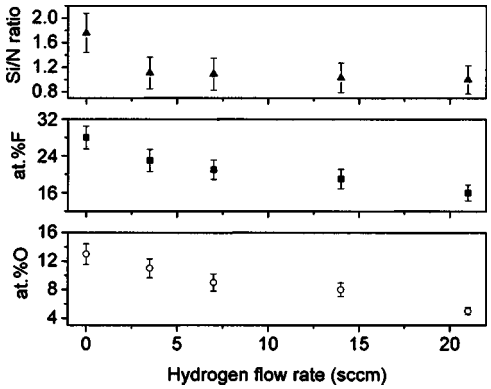

FIG. 7. Plots of Si/N ratio (upper), at. % F (middle) and at. % O (bottom), vs hydrogen flow rate used during deposition.

The concentrations of Si–H and N–H bonds incorporated in the films were calculated using the formula[43,47]

$$[H]_i = \frac{2.303}{d} K_i \int A_i(\omega) d\omega, \tag{1}$$

where $[H]_i$ is the concentration of hydrogen bonded to silicon or nitrogen, the subindex i is used to distinguish between Si–H and N–H bonds, $A_i(\omega)$ is the absorbance produced by the corresponding bond as a function of the wave number ω, d is the thickness of the film, and K_i is a constant, which takes the values; $K_{SiH}=7.1\times10^{16}$ cm^{-1} and $K_{NH}=8.2\times10^{16}$ cm^{-1}.[43] The concentrations of Si–H and N–H bonds calculated by this procedure, as a function of hydrogen flow rate, are shown in Fig. 5. This figure shows that the N–H bond concentration increases asymptotically toward $\sim5.5\times10^{21}$ cm^{-3}, as the hydrogen flow rate increases from 0 to 21 sccm. On the other hand, the concentration of Si–H bonds is quite low (below 1.2×10^{21} cm^{-3}) for films deposited without hydrogen and at 3.5 sccm, and it is below the FTIR detection limit ($\sim1\%$) for films deposited at higher hydrogen flow rates.

Figure 6 shows the $^{19}F(p,\alpha\gamma)^{16}O$ RNR excitation curves obtained from F-containing Si_3N_4 films. These curves correspond to the amount of fluorine atoms as a function of the film depth. The F depth profile is quite flat for most of the films, except for the film deposited without hydrogen, in which a surface fluorine depletion is observed. The behavior of the total amount of F in the films as a function of hydrogen flow rate is depicted in Fig. 7. One can observe from this figure that the F content decreases as the H_2 flow rate increases. The relative content of Si, N, F, and O atoms in the films was determined by RBS using a ^{4}He beam at 3.05 MeV, which occurs for the elastic $^{16}O(\alpha,\alpha)^{16}O$ scattering resonance which intensifies the oxygen signal. The RBS results indicate that the Si/N ratio first decreases and then it is practically constant, meanwhile the oxygen content decreases systematically as the H_2 flow rate increases (see Fig. 7).

Figure 8 shows the typical current-voltage characteristics of MIS structures incorporating fluorinated silicon nitride films deposited under three different hydrogen flow rate conditions; 0, 7, and 21 sccm. The leakage current for the silicon nitride film deposited without hydrogen is quite high, however, it is significantly lower for the films deposited with hydrogen. The lowest leakage current corresponds to films deposited at the highest hydrogen flow rate (21 sccm), and it is lower than 1×10^{-5} A/cm^2 for electric fields as high as 7 MV/cm.

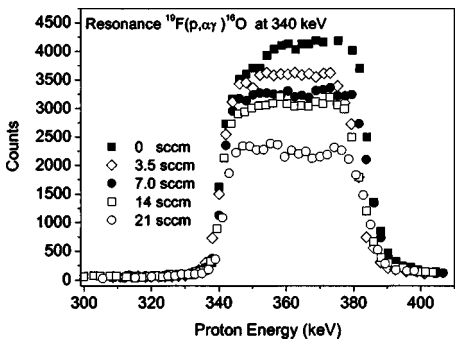

FIG. 6. RNRA spectra of fluorine resonance at 340 keV obtained from films deposited under different hydrogen flow rates.

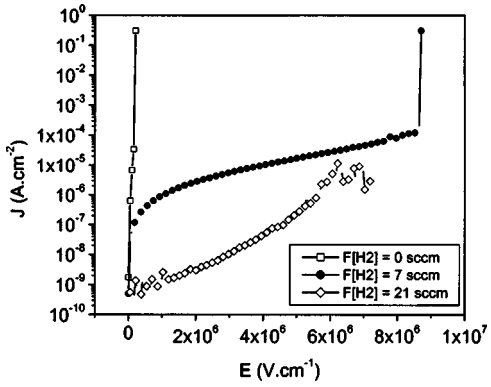

FIG. 8. Current density–electric-field characteristic for MIS structures constructed with fluorinated silicon-nitride films deposited with different hydrogen flow rates.

IV. DISCUSSION

Our results show that hydrogen flow rate has an important effect on the deposition rate, composition, structural, chemical, and electrical properties of the fluorinated silicon nitride films. We can explain most of these results on the basis of a comparative analysis of some of the simplest overall possible reaction pathways for film deposition, for each case; with and without hydrogen.

Given the gas feed configuration in our RPECVD system, when no hydrogen is used during deposition, some of the possible overall reaction pathways for film formation can be the following;

$$\text{plasma zone:} \quad (N_2 + Ar)^* \rightarrow N_2^* + Ar^*, \tag{2}$$

$$\text{downstream:} \quad Ar^* + N_2^* + SiF_4 \rightarrow SiFN(s) + NF_3 + Ar, \tag{3}$$

$$Ar^* + SiF_4 \rightarrow SiF(s) + F_2 + F + Ar, \tag{4}$$

where the asterisks indicate the plasma excitation process or excited state of the atoms and/or radicals. Reaction (2) indicates that N_2 and Ar are excited in the remote plasma zone, producing energetic Ar metastables (Ar^*) and nitrogen excited species (N_2^*). Reaction (3) indicates that at the outside plasma zone, the SiF_4 molecules introduced downstream through the gas dispersal ring are dissociated by the activated species from the plasma zone, and that the growth of the solid film [SiNF(s) or SiN_x:F(s)] occurs through the heterogeneous reactions between SiF radicals and N radicals on the substrate surface. Reaction (4) indicates that some of the SiF radicals produced by impact of Ar^* with the SiF_4 can react with themselves, forming a solid phase of fluorinated silicon [SiF(s) or Si:F(s)] on the substrate surface.

When hydrogen molecules are added to the downstream region, the reactions in the plasma zone are the same as Eq. (2), but the reactions outside the plasma region are modified. So, in this case some possible reactions can be described by

$$\text{downstream:} \quad Ar^* + N_2^* + SiF_4 + H_2 \rightarrow SiN_2(s) + 2HF + F_2 + Ar, \tag{5}$$

$$Ar^* + SiF_4 + H_2 \rightarrow Si + 2HF + F_2 + Ar. \tag{6}$$

In Eqs. (5) and (6), it has been ideally assumed that hydrogen atoms are 100% effective in removing fluorine atoms from the growing film. Although in practice this idealization does not occur, it has been done so in order to emphasize that hydrogen atoms have the ability of removing fluorine atoms from the growing film, forming volatile HF.[48,49]

As Fig. 1 shows, we obtained the highest film deposition rate without adding any hydrogen to the remote plasma activated reactions, and the film deposition rate decreases as H_2 is added to the reactions. This behavior is opposite to that found in the past by Fujita for films deposited from the same $SiF_4/N_2/H_2$ mixture.[22] Using a conventional PECVD discharge Fujita found that film deposition does not take place if hydrogen is not included in the plasma reactions and that film deposition rate increases with hydrogen addition. This means that the simple criteria used by Fujita to explain the absence of film growth without hydrogen, based on the hierarchy of diatomic bond energies (5.57 eV for Si–F, 5.2 eV for Si–N),[22] is insufficient to explain our experimental results, and therefore other growing mechanisms and processes must be taken into account.

As it has been reported in a recent study on the gas phase and surface chemistry of SiF_4 and SiF_4/H_2 plasmas interacting with Si substrates, there are a variety of plasma-surface processes in this system, such as radical-surface reactions, radical-radical gas phase reactions, ion bombardment, which may contribute to film deposit, etching, and/or only F atom incorporation.[49] The balance between film growth and substrate etching in these fluorosilane systems depends on the concentration of the different chemical species generated by the plasma reactions and their interaction with the substrate being processed, which in turn depend on experimental conditions such as feed gas composition, plasma power, pressure, etc. Some specific conclusions[49] which are useful for the discussion of our deposition process are the following: (i) the equilibrium between etching and deposition processes can be monitored by film deposition rate, which is inversely proportional to the SiF_2 gas phase density, (ii) SiF_2 and SiF_4 are the main volatile product of Si etching by F atoms, (iii) SiF is the main film deposition precursor and the contribution of this radical to film growth is related to both gas-phase density and to sticking probability, (iv) when H_2 is included in the reactions, volatile HF is produced by gas phase reactions of H atoms with SiF_x ($x=1,2,3,4$) radical. In addition to H atom scavenging of F atoms, which inhibit the Si etching, new deposition precursors are formed.

Based on the above-mentioned study and given the high deposition rate of films deposited without hydrogen we can conclude that in this case and under our experimental conditions (high remote plasma power, and low pressure), the production of fluorine-silicon film deposition precursors predominates over that of etching and/or volatile species which do not form a deposit. Thus in the absence of hydrogen the deposit can proceed through reactions between SiF radicals and the nitrogen excited species, N_2^*, or other SiF radicals [see Eqs. (3) and (4)], and there is well expected incorporation of great amounts of silicon-fluorine radicals in the films. This explains why films deposited without hydrogen have the highest amount of fluorine atoms incorporated and the lowest refractive index (see Figs. 1, 6, and 7). Given the high fluorine content, and since F atoms tend to form terminal bonds (they join with only one atom), it is well expected that the films will result with an open structure (low density),[27,31,33] and with a fluorine terminated surface, which is consistent with its high chemical etch rate (see Fig. 2). As it has been reported previously, when a porous and fluorine terminated silicon or silicon nitride surface is exposed to the ambient moisture, it is oxidatively attacked through penetration of oxygen and water molecules in its network, losing fluorine through the formation of volatile HF.[49,50] This explains the fluorine surface depletion observed in the RNR

spectra shown in Fig. 6 corresponding to the film deposited without hydrogen, and the high oxygen content in this film (Fig. 7). The contradictory appearance of Si–H and N–H bonds found in the IR spectrum of the film deposited without hydrogen (Figs. 3 and 5) can also be explained in terms of a complicated postdeposition hydrolization process generated by the atmospheric moisture, where the final products are not only Si–O bonds but also N–H and Si–H bonds. The fact that the IR characteristics and refractive index of these films (and all the other) do not change after being exposed to the ambient moisture and immersion in deionized water means that the hydrolyzation/oxidation occur almost instantaneously when the films are withdrawn from the reactor and that this process saturates rapidly because it only removes the weakly bonded fluorine surface atoms but leaves intact the major proportion of F atoms, which are forming strong and stable bonds. However, a deep explanation of how the hydrolyzation and stabilization occur is out of the scope of this work.

The large shift of the fundamental Si–N absorption peak ($950\ cm^{-1}$) for the film deposited without hydrogen compared with that of hydrogenated silicon-nitride films ($850\ cm^{-1}$) is consistent with its high fluorine content (28% at.) and it is supposed to be caused by the enhancement of the elastic constant of the Si–N bonds where there is a back-bonded F atom which leaves more positive partial charge in the Si atom.[22]

The incorporation of high amounts of Si–F bonds in the film deposited without hydrogen is also consistent with its high Si/N ratio. A theoretical rough estimation of the Si/N ratio for the as-deposited film under this condition can be made if we assume that the F atoms substitute for the N atoms in the fundamental $Si-N_4$ tetrahedral units which form the ideal Si_3N_4 random network (where each nitrogen atom is bonded to three silicon atoms). For example, if we assume that only one fluorine atom is incorporated in each of the $Si-N_4$ tetrahedral, assuming that each of the remaining N atoms continue bonded to three silicon atoms, the composition would be $SiN_{3/3}F$ or SiNF. In this case the percentage of fluorine atoms would be 33.33% and the ratio $Si/N=1$. Thus the fact that the experimental Si/N ratio is much higher than 1 (~ 1.68) indicates that the as-deposited film must contain a higher fluorine content (SiN_xF_y with $x<1$, $y>1$) and/or that there are some Si–Si bonds incorporated in the film. Then, the lower percentage of fluorine atoms experimentally found for this film after being exposed to the ambient moisture ($\sim 28\%$), can be explained in terms of the fluorine loss through HF formation by the above-mentioned hydrolyzation effect.

The reduction in film deposition rate as H_2 is added to the remote plasma activated reactions, shown in Fig. 2, can be speculatively associated to the dilution of the SiF_4 gas, produced by the increase in the partial pressure of hydrogen, because when hydrogen is added to the downstream region a fraction of the energetic species (Ar^*, N_2^*, etc.) coming from the plasma zone will transfer its energy to the H_2 molecules to dissociate them instead of dissociating the SiF_4 molecules. This will reduce the amount of SiF radicals contributing to the film growth, and consequently the film growth rate will be decreased. Equations (5) and (6) also show that atomic hydrogen will extract fluorine from the reactive species through the formation of HF. This explains the reduction observed in the fluorine content (Figs. 6 and 7), the shift of the main Si–N IR absorption peak toward lower wave numbers (Fig. 4), and the increase in the refractive index (Fig. 1) of the films as the hydrogen flow rate is increased. The reduction in the fluorine content of the films also gives rise to a less open structure with the consequent diminution in their chemical etch rate as the hydrogen flow rate increases (Fig. 2).

The fact that the concentration of N–H bonds increases while that of the Si–H decreases (toward undetectable limits) as the hydrogen flow rate increases (see Fig. 5) indicates that the N–H bonds are formed during the deposition of these films, meanwhile the Si–H bonds are not formed *in situ* but after exposing the films to the ambient moisture. The possibility that the Si–H bonds be formed during the deposition process is discarded due to the low bonding energy of Si–H (3.24 eV) compared to that of the N–H (3.73 eV) and Si–F (5.59 eV) bonds.[51] It is well expected that the films become less silicon rich when hydrogen is added to the reactions because the extraction of fluorine from forming the Si–F bonds allows the formation of more Si–N bonds. However, since the increase in the hydrogen flow rate is also accompanied by an increase in the amount of N–H bonds, which has the contrary effect of inhibiting the formation of N–Si bonds, both processes can give rise to the almost null variation in the Si/N ratio of films deposited with H_2 flow rates distinct of zero, observed in Fig. 7. The value of this ratio ($Si/N=1$) for the films deposited with hydrogen, corresponds to a silicon rich composition, which may be indicative that they contain a certain amount of Si–Si bonds. The reduction in the oxygen content as the hydrogen flow rate increases indicates that the oxygen is incorporated in the films after deposition by the hydrolyzation process, since this effect is weakened as a result of the fluorine content reduction. The low refractive index of these fluorinated silicon nitride films, compared with that for Si_3N_4 (2.0), can be due not only to the lower polarizability of the F ($0.557\times10^{-24}\ cm^3$) (Ref. 34) atoms compared with that of the N ($1.1\times10^{-24}\ cm^3$) (Ref. 34) atoms, but also to the opening of the network produced by the presence of the terminal Si–F bonds, as has been proposed in other previous works.[31,32] Based on this explanation, the increase in the refractive index as the hydrogen flow rate increases is well expected due to the reduction in the fluorine content. It should be cleared that the density of our films, determined from RBS and film thickness measurements, decreases from 2.6 to 2.5 gr/cm^3 as the fluorine content increases from its minimum (16 at. %) to its maximum (27 at. %) value. The low-density values found for our films, compared with that for Si_3N_4 ($3.5\ gr/cm^3$), are similar to those reported for fluorinated silicon nitride films prepared from other mixtures and/or processes,[27,31,33] and they give some support to the argument of the opening of the film network as a result of

fluorine incorporation. The small decrease in the density of these films, as a function of fluorine content, can be explained in terms of a quasibalance between two opposite effects: the network opening and the increment in the mass of the films due to the increase in their Si content (see Fig. 7).

The very poor electrical properties of the film deposited without hydrogen is associated to both its highly silicon-rich composition and the high content of Si–H bonds, which promotes an increased probability for Poole-Frenkel trap emission.[52] The remarkable improvement in the electrical properties of the fluorinated silicon nitride films as the hydrogen flow rate increases (Fig. 8) can be explained as a result of the reduction in the fluorine content and elimination of Si–H bonds, which allows a film composition less silicon rich with reduced charge transport rates.[52]

V. CONCLUSIONS

Fluorinated silicon nitride films have been grown by RPECVD at 250 °C from $Ar/SiF_4/N_2/H_2$ mixtures, under various hydrogen flow rates. Our experimental results show that fluorinated silicon nitride films can be deposited without adding any hydrogen to the plasma reactions. The deposition rate of films deposited without hydrogen was the highest, however, they also resulted with the highest fluorine content and silicon-rich composition. The Si–H and N–H bonds, as well as oxygen found in these films, indicate that these films suffer a complex post-deposition hydrolyzation, which is very probably a consequence of the excess of fluorine content. These films also resulted with very poor insulating electrical properties. The main effect of adding hydrogen to the deposition process is to improve the chemical stability and dielectric properties of the films through the reduction in the amount of fluorine incorporated in the films, although it also reduces the deposition rate. Although the Si/N ratio of films deposited with hydrogen is lower than that for films deposited without hydrogen, this ratio remains constant as the hydrogen flow rate increases in the range studied. This demonstrates that our approach of using a hydrogen source (H_2) separated from the nitrogen source (N_2), is effective for controlling the fluorine incorporation in the RPECVD films, independently of the Si/N ratio. The purpose of Si–H bonds elimination from the silicon nitride films was also achieved under our approach, since the use of hydrogen flow rates higher than 3.5 sccm produces films free of these bonds. The maximum concentration of N–H bonds incorporated in all these films was relatively low ($\sim 5\times 10^{21}$ cm^{-3}). Fluorinated silicon-nitride films deposited with the highest hydrogen flow rate used in this work (21 sccm) were the most chemically stable and had the better dielectric properties.

ACKNOWLEDGMENTS

The authors would like to thank S. Jiménez, M. A. Canseco, and J. Camacho from the Instituto de Investigaciones en Materiales, and Rafael Macías, J. C. Pineda, K. López, and F. J. Jaimes from the Instituto de Física, UNAM for technical assistance. This work has been partially supported by Consejo Nacional de Ciencia y Tecnología (CONACyT) of México under Project No. 26423-A and DGAPA-UNAM under PAPIIT Project No. IN119904.

[1] G. Lucovsky, IBM J. Res. Dev. **43**, 301 (1999).
[2] C. Y. Chang and S. M. Sze, *ULSI Technology* (Wiley International, New York, 2000).
[3] C. Boheme and G. Lucovsky, J. Appl. Phys. **88**, 6055 (2000).
[4] A. R. Merticaru, A. J. Mouthaan, and F. G. Kuper, Thin Solid Films **427**, 60 (2003).
[5] G. Santana and A. Morales-Acevedo, Sol. Energy Mater. Sol. Cells **60**, 135 (2000).
[6] *Plasma Deposition of Amorphous Silicon-Based Materials*, edited by G. Bruno, P. Capezzuto, and A. Madan (Academic, Boston, 1995).
[7] R. B. Beck, M. Giedz, A. Wojtkiewicz, A. Kudla, and A. Jacubowski, Vacuum **70**, 323 (2003).
[8] S. Liao, C. H. Lin, and S. C. Lee, Appl. Phys. Lett. **65**, 2229 (1994).
[9] Y. Kuo and H. H. Lee, Vacuum **66**, 299 (2002).
[10] M. Bose, D. K. Basa, and D. N. Bose, Mater. Lett. **48**, 336 (2001).
[11] G. Beshkov, S. Lei, V. Lazarova, N. Nedev, and S. S. Georgiev, Vacuum **69**, 301 (2003).
[12] B. Kim, D. W. Kim, and S. S. Han, Vacuum **72**, 385 (2004).
[13] G. Lucovsky and D. Tsu, J. Cryst. Growth **86**, 804 (1988).
[14] Y. B. Park and S. W. Rhee, J. Mater. Sci.: Mater. Electron. **12**, 515 (2001).
[15] V. Misra, H. Lazar, Z. Wang, Y. Wu, H. Niimi, G. Lucovsky, J. J. Wortman, and J. R. Hauser, J. Vac. Sci. Technol. B **17**, 1836 (1999).
[16] J. C. Barbour, H. J. Stein, O. A. Popov, M. Yoder, and C. A. Outten, J. Vac. Sci. Technol. A **9**, 480 (1991).
[17] C. Doughty, D. C. Knick, J. B. Bailey, and J. E. Spencer, J. Vac. Sci. Technol. A **17**, 2612 (1999).
[18] M. C. Hugon, F. Delmotte, B. Agius, and J. L. Courant, J. Vac. Sci. Technol. A **15**, 3143 (1997).
[19] C. Hodson, Plasma News-Oxford Instruments Plasma Technology, January 4 (2004).
[20] S. Fujita, H. Toyoshima, T. Ohishi, and A. Sasaki, Jpn. J. Appl. Phys., Part 2 **23**, L144 (1984).
[21] S. Fujita, H. Toyoshima, T. Ohishi, and A. Sasaki, Jpn. J. Appl. Phys., Part 2 **23**, L268 (1984).
[22] S. Fujita and A. Sasaki, J. Electrochem. Soc. **135**, 2566 (1988).
[23] N. Watanabe, M. Yoshida, Y. C. Jiang, T. Nomoto, and I. Abiko, Jpn. J. Appl. Phys., Part 2 **30**, L619 (1991).
[24] G. Cicala, G. Bruno, P. Capezzuto, and M. Losurdo, in *Laser Ablation in Materials Processing: Fundamentals and Applications*, edited by B. Braren, J. Dubowski, and D. Norton, Mater. Res. Soc. Symp. Proc. (Materials Research Society, Pittsburgh, 1993), p. 27.
[25] H. Ohta, M. Hori, and T. Goto, J. Appl. Phys. **90**, 1955 (2001).
[26] L. S. Zambon and R. D. Mansano, Vacuum **71**, 439 (2003).
[27] J. Fandiño, A. Ortiz, L. Rodríguez-Fernández, and J. C. Alonso, J. Vac. Sci. Technol. A **22**, 570 (2004).
[28] C. P. Chang, D. L. Flamm, D. E. Ibbotson, and J. A. Mucha, J. Appl. Phys. **62**, 1406 (1987).
[29] C. P. Chang, D. L. Flamm, D. E. Ibbotson, and J. A. Mucha, J. Vac. Sci. Technol. B **6**, 524 (1988).
[30] R. E. Livengood, M. A. Petrich, D. W. Hess, and J. A. Reimer, J. Appl. Phys. **63**, 2651 (1988).
[31] C. S. Pai, C. P. Chang, F. A. Baiocchi, and J. Swiderski, J. Appl. Phys. **68**, 2442 (1990).
[32] O. Sanchez, C. Gómez-Alexandre, and C. Palacio, J. Vac. Sci. Technol. B **11**, 66 (1993).
[33] B. J. Jun, J. S. Lee, and D. W. Kim, J. Mater. Res. **14**, 995 (1999).
[34] J. A. Kerr and D. W. Stockes, in *Handbook of Chemistry and Physics*, 83rd ed., edited by D. R. Lide (Academic, New York, 2002).
[35] J. P. Hirvonen, in *Handbook of Modern Ion Beam Materials Analysis*, edited by J. R. Tesmer and M. Nastasi (Materials Research Society, Pittsburgh, 1995), p. 176.
[36] O. G. de Lucio and J. Miranda, Instrum. Dev. **4**, 12 (1999).
[37] J. F. Ziegler, J. P. Biersack, and U. Littmark, *The Stopping and Range of Ions in Solids* (Pergamon, New York, 1985), Vol. 1.
[38] G. Vizkelethy, P. Revesz, J. W. Mayer, and Jian Li, Surf. Interface Anal. **20**, 309 (1993).
[39] L. R. Doolittle, Nucl. Instrum. Methods Phys. Res. B **9**, 344 (1985).
[40] D. V. Tsu, G. Lucovsky, and M. J. Mantini, Phys. Rev. B **33**, 7069

(1986).
[41]C. J. Fang, L. Ley, H. R. Shanks, K. J. Gruntz, and M. Cardona, Phys. Rev. B **22**, 6140 (1980).
[42]K. Yamamoto, M. Tsuji, K. Washio, H. Kasahara, and K. Abe, J. Phys. Soc. Jpn. **52**, 925 (1983).
[43]D. V. Tsu and G. Lucovsky, J. Vac. Sci. Technol. A **4**, 480 (1986).
[44]G. Lucovsky and D. V. Tsu, J. Vac. Sci. Technol. A **5**, 2231 (1987).
[45]V. Pankov, J. C. Alonso, and A. Ortiz, J. Appl. Phys. **86**, 275 (1999).
[46]J. A. Theil, D. V. Tsu, M. W. Watkins, S. S. Kim, and G. Lucovsky, J. Vac. Sci. Technol. A **8**, 1374 (1990).
[47]A. C. Adams, Solid State Technol. **26**, 135 (1983).
[48]G. Bruno, P. Capezzuto, and G. Cicala, J. Appl. Phys. **69**, 7256 (1991).
[49]K. L. Williams, C. I. Butoi, and E. R. Fisher, J. Vac. Sci. Technol. A **21**, 1688 (2003).
[50]R. A. Haring and M. Liehr, J. Vac. Sci. Technol. A **10**, 802 (1992).
[51]R. T. Sanderson, *Chemical Bonds and Bond Energy*, 2nd ed. (Academic, New York, 1976).
[52]S. Habermel and C. Carmignani, Appl. Phys. Lett. **80**, 261 (2002).